Effects of backward-propagating waves and lumped mirror losses on self-induced transparency modelocking in quantum cascade lasers

Muhammad Anisuzzaman Talukder[a] and Curtis R. Menyuk[b]
Department of Computer Science and Electrical Engineering, University of Maryland, Baltimore County 1000 Hilltop Circle, Baltimore, Maryland 21250, USA

(Received 20 June 2009; accepted 28 July 2009; published online 20 August 2009)

Work to date on self-induced transparency modelocking in quantum cascade lasers (QCLs) has neglected backward-propagating waves and lumped mirror losses. In this work, we remove these unrealistic assumptions. The qualitative features of the modelocking are unaffected by this improvement in the model, but the parameter regime in which stable modelocked pulses may be found is reduced. This reduction is due to incomplete gain recovery near the edges of the QCL when pulses pass through after reflecting from the mirrors, coincident with the loss of pulse energy at the mirrors. Spatial hole burning is observed in parameter regimes in which continuous waves can grow, but it does not affect the stability of the modelocking. © *2009 American Institute of Physics*. [DOI: 10.1063/1.3206741]

Conventional passive modelocking[1,2] is difficult to achieve in quantum cascade lasers[3] due to their narrow linewidths and fast recovery times. Gain bandwidths in quantum cascade lasers (QCLs) are narrow because QCLs are intersubband transition devices and they have long coherence times (T_2) for semiconductor lasers, on the order of 100–200 fs.[4] The coherence time is mainly determined by intrasubband carrier-carrier, carrier-LO phonon, and carrier-interface roughness scattering.[5,6] The gain recovery time (T_1) in QCLs is short compared to other semiconductor lasers, on the order of a picosecond, mainly due to carrier-transport through the quantum cascade structure by coherent tunneling and incoherent scattering mechanisms.[7] In conventional passive modelocking, gain bandwidths that are significantly larger than the pulse bandwidths are required. Also a saturable gain, with a recovery time that is long compared to round-trip time (T_{rt}) is required in order to suppress continuous waves that may lead to instability due to the Risken–Nummedal–Graham–Haken effect.[8] However, typical gain recovery times in QCLs are shorter than the round-trip times. Thus, conventional passive modelocking cannot work in QCLs that operate in a standard parameter regime. Recently, in Refs. 9 and 10, we showed that the self-induced transparency (SIT) effect[11,12] can be used to modelock QCLs. In order to achieve modelocking, QCLs should have absorbing periods interleaved with gain periods, and the absorbing periods should have a dipole moment μ_a approximately twice as large as the dipole moment in the gain periods μ_g, so that π pulses in the gain periods are also 2π pulses in the absorbing periods. We have demonstrated QCL structures[13] that satisfy the requirements of SIT modelocking, and our analytical and computational studies showed that SIT modelocking for QCLs is robust.[10,14] Previously, we have used the Maxwell–Bloch equations, applied to a simple two-level system,[15,16] to model both the gain and absorbing periods, in which all spatial inhomogeneity was ignored. In particular, the large lumped mirror losses were averaged over the propagation. We also only considered the waves that propagate in a single direction. A unidirectional propagation model for the evolution of modelocked pulses is a standard approach in the literature and has been extensively used.[17] However, when continuous waves experience gain, the forward- and backward-propagating waves produce standing waves, which can interfere nonlinearly due to the small values of T_1. As a result, Wang *et al.*[18] and Gordon *et al.*[19] observed spatial hole burning (SHB) in conventional QCLs with an input current set above threshold.

In this letter, we will show that backward-propagating waves do not affect the stability of SIT modelocking. SIT modelocking is only stable when backward-going continuous waves are suppressed and hence cannot interact with forward-going waves. By contrast, the lumped losses at the mirrors do affect the stability, due to the incomplete gain recovery that the pulses experience after reflecting from the mirrors, coincident with their loss of energy at the mirrors.

When the electric field propagates in only one direction, so that there is no interference, and we ignore spatial inhomogeneity, the dynamics in a QCL having absorbing periods in addition to gain periods can be described by the Maxwell–Bloch equations in the two-level approximation,[9]

$$\frac{n}{c}\frac{\partial E}{\partial t}+\frac{\partial E}{\partial z}=-i\sum_{x=a,g}\frac{kN_x\Gamma_x\mu_x}{2\epsilon_0 n^2}\eta_x-\frac{1}{2}l_u E, \tag{1a}$$

$$\frac{\partial \eta_{g,a}}{\partial t}=\frac{i\mu_{g,a}}{2\hbar}\Delta_{g,a}E-\frac{\eta_{g,a}}{T_{2g,a}}, \tag{1b}$$

$$\frac{\partial \Delta_{g,a}}{\partial t}=\frac{i\mu_{g,a}}{\hbar}\eta_{g,a}E^*-\frac{i\mu_{g,a}}{\hbar}\eta^*_{g,a}E+\frac{\Delta_{g,a0}-\Delta_{g,a}}{T_{1g,a}}, \tag{1c}$$

where the subscripts g and a in Eqs. (1b) and (1c) represent gain and absorption, respectively. The independent variables z and t are length along the light-propagation axis of the QCL and time. The dependent variables E, $\eta_{g,a}$, and $\Delta_{g,a}$ refer to the envelopes of the electric field, gain polarization, and gain inversion. The parameters $\Delta_{g0}\simeq 1.0$ and $\Delta_{a0}\simeq -1.0$ refer to the equilibrium inversion away from the modelocked pulse. The parameters n and c denote the index of refraction and the speed of light. The parameters $N_{g,a}\Gamma_{g,a}$

[a]Electronic mail: anisuzzaman@umbc.edu.
[b]Electronic mail: menyuk@umbc.edu.

denote the effective electron density multiplied by the overlap factor. The parameters k, l_u, ϵ_0, and $\hbar$ denote the wavenumber, the average linear loss including mirror loss, the vacuum dielectric permittivity, and Planck's constant.

If counterpropagating waves are taken into account, and we take into account the lumped mirror losses, then the dynamics can be described by

$$\frac{n}{c}\frac{\partial E_\pm}{\partial t} + \frac{\partial E_\pm}{\partial z} = -i\sum_{x=a,g}\frac{kN_x\Gamma_x\mu_x}{2\epsilon_0 n^2}\eta_{x\pm} - \frac{1}{2}l_b E_\pm, \tag{2a}$$

$$\frac{\partial \eta_{g,a\pm}}{\partial t} = i\frac{\mu_{g,a}}{2\hbar}(\Delta_{g,a}E_\pm + \Delta^{\pm}_{2g,a}E_{\mp}) - \frac{\eta_{g,a\pm}}{T_{2g,a}}, \tag{2b}$$

$$\frac{\partial \Delta_{g,a}}{\partial t} = i\frac{\mu_{g,a}}{\hbar}(\eta_{g,a+}E^*_+ + \eta_{g,a-}E^*_- - \text{c.c.}) + \frac{\Delta_{g,a0} - \Delta_{g,a}}{T_{1g,a}}, \tag{2c}$$

$$\frac{\partial \Delta^{\pm}_{2g,a}}{\partial t} = \pm i\frac{\mu_{g,a}}{\hbar}(E^*_+\eta_{g,a-} - \eta^*_{g,a+}E_-) - \frac{\Delta^{\pm}_{2g,a}}{T_{1g,a}}, \tag{2d}$$

where the variables, constants, and subscripts are the same as in Eq. (1) except that $\Delta_{2g,a}$ refers to the inversion grating. The quantities with + (−) subscripts represent waves traveling in the positive (negative) z-direction. Equations (2c) and (2d) allow us to take SHB into account. The linear loss l_b in Eq. (2) only includes the loss in the medium. Mirror losses are taken into account by the boundary conditions. QCLs have cleaved facets, and the reflection coefficients at the edges depend on the refractive index difference between the laser medium and air, i.e., $r_-=r_+=(n-1)/(n+1)$, where r_- and r_+ are the reflection coefficients at the two interfaces. The notation closely follows that of Wang *et al.*[18] and Gordon *et al.*,[19] with the differences that we have an absorbing as well as a gain medium.

The gain per unit length (g) from the gain periods of the QCL and the absorption per unit length (a) from the absorbing periods are given by[9]

$$g = \frac{kN_g\Gamma_g\mu_g^2 T_{2g}}{2\epsilon_0 n^2\hbar}, \quad a = \frac{kN_a\Gamma_a\mu_a^2 T_{2a}}{2\epsilon_0 n^2\hbar}. \tag{3}$$

We present the results in terms of normalized gain ($\bar{g}$) and absorption ($\bar{a}$) coefficients. Gain and absorption coefficients are normalized by average loss per unit length, which is l_u when we solve Eq. (1) and is $l_b - \ln r_-/L - \ln r_+/L$ when we solve Eq. (2). Here, we use L to denote the cavity length.

An extensive computational analysis of SIT modelocking using Eq. (1) has been presented in Ref. 10. Here, we analyze SIT modelocking by computationally solving Eq. (2). We assume that a resonant pulse of hyperbolic-secant shape and a π pulse in the gain medium are injected into the QCL structure from an external source. We note that since continuous waves must be suppressed, this laser will not self-start. Our computational results show that stable modelocked solutions exist. An initially broad pulse becomes narrower and evolves toward a fixed profile intensity after each round trip. We show the pulse evolution in a 3-mm-long QCL cavity in Fig. 1. In this example, we set $\bar{g}=3.5$ and $\bar{a}=2.8$. An initial pulse of 100 fs duration (full width at half maximum/1.763) narrows down to ~65 fs. The pulse narrowing when we solve Eq. (2) is less than when we solve Eq. (1). With the same parameters and initial conditions as in Fig. 1, the stable pulse duration is only ~43.5 fs, when solving Eq. (1).

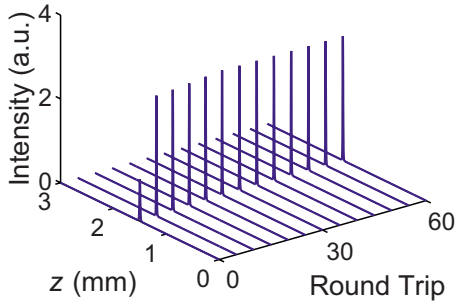

FIG. 1. (Color online) Modelocked pulse evolution. We set $T_{1g}=T_{1a}\equiv T_1$, $T_{2g}=T_{2a}\equiv T_2$, and $T_1/T_2=10$ with $T_2=100$ fs.

Figure 2 compares the stability limits of $\bar{g}$ and $\bar{a}$ for SIT modelocking when we solve Eq. (1) and when we solve Eq. (2). The bottom black solid line shows the lower stability limit in both cases. This boundary is set by the growth of continuous waves. If the lasers are operated with parameters set below this boundary, continuous waves are unstable, and multiple pulses may form due to the Risken–Nummedal–Graham–Haken effect. The upper lines show the upper stability limits of $\bar{a}$ and are set by the losses. If the laser is operated with parameters set above these lines, pulses damp. The upper limiting values of $\bar{a}$ are smaller when we solve Eq. (2) than when we solve Eq. (1) due to the lumped mirror losses and the delay in the gain recovery when pulses reflect from the mirrors. Pulses lose a significant amount of energy (~50%) at the QCL mirrors before bouncing back for another passage through the laser. Ideally, the absorption should decrease and the gain should increase in order for the pulse to grow to a sustainable intensity. However, just the opposite occurs. When the pulses bounce back from the cavity edges, the inversion $\Delta_{g,a}$ will not have regained its equilibrium value before the pulse passes through again. When QCLs operate below the lower stability limit in $\bar{a}$, continuous waves are unstable, so that multiple pulses are created and interfere each other, and we observe SHB in some parameter regimes. However, if QCLs are operated with $\bar{a}$ above the lower stability limit, continuous wave growth is suppressed by the absorbing layers, and no SHB is observed.

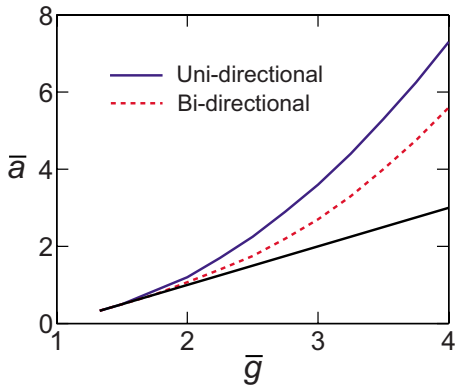

FIG. 2. (Color online) Stability limits of normalized gain ($\bar{g}$) vs normalized absorption ($\bar{a}$) coefficients. We set $T_{1g}=T_{1a}\equiv T_1$, $T_{2g}=T_{2a}\equiv T_2$, and $T_1/T_2=10$ with $T_2=100$ fs. The upper curves are the upper limiting values of $\bar{a}$. The bottom black line is the limiting values for continuous wave (cw) growth for both cases.

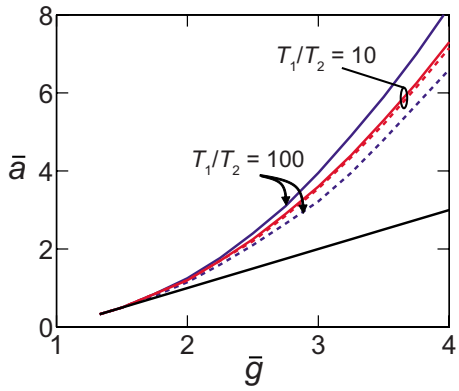

FIG. 3. (Color online) Stability limits for different T_1/T_2 values with $r_-=1$ and $r_+=1$. Solid lines show solutions of Eq. (1), while dashed lines show solutions of Eq. (2).

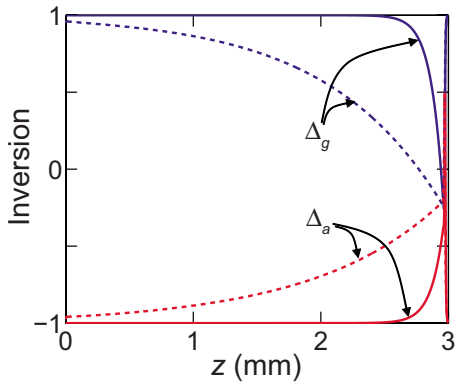

FIG. 4. (Color online) Population inversion in the cavity. The solid lines are for $T_1/T_2=10$ and the dashed lines are for $T_1/T_2=100$.

In Fig. 3, we show the effect of the gain recovery time on the upper stability limit in $\bar{a}$. We set $r_-=r_+=1$ so that we can observe the change in stability that is due only to the delay in the gain recovery. We assume $T_{1g}=T_{1a}\equiv T_1$ and $T_{2g}=T_{2a}\equiv T_2$. As expected, the upper limit in $\bar{a}$ is lower when we solve Eq. (2), than it is when we solve Eq. (1), even though there are no mirror losses. When we solve Eq. (1), the upper stability limit in $\bar{a}$ increases, whereas it decreases when we solve Eq. (2). However, when $T_1/T_2=10$ with $T_2=100$ fs, the gain recovery time T_1 is only 1 ps, which is a typical value obtained in QCLs, and is very short compared to the cavity round-trip time of ~ 50 ps. Therefore, the population inversion can recover its equilibrium value before the pulse passes through after reflecting from the mirrors, except in a small region near the edges of the QCL. The instantaneous population inversions for both the gain and absorbing media are drawn in Fig. 4 at different points in the cavity when the pulse bounces back from the right edge. Figure 4 shows that when T_1/T_2 become large, i.e., $T_1/T_2=100$ with $T_2=100$ fs, the population inversion at the left edge has not recovered even when the pulse reaches the right edge.

In conclusion, we have shown that SIT modelocking is stable in QCLs when we take into account realistic, lumped mirror losses, and backward-propagating waves. However, the stable parameter regime is reduced. Incomplete gain recovery at the QCL edges, when the pulses pass through after reflecting from the mirrors, along with mirror losses, is largely responsible for this reduction. Since continuous waves are suppressed in the stable operating regime, SHB does not appear in this regime. It does appear when $\bar{a}$ is below the stable operating limit.

[1]M. H. Crowell, IEEE J. Quantum Electron. **1**, 12 (1965).
[2]T. Uchida and A. Ueki, IEEE J. Quantum Electron. **3**, 17 (1967).
[3]J. Faist, F. Capasso, D. Sivco, C. Sirtori, A. Hutchinson, and A. Cho, Science **264**, 553 (1994).
[4]C. Sirtori and R. Teissier, in *Intersubband Transitions in Quantum Structures*, edited by R. Paiella (McGraw-Hill, New York, 2006).
[5]M. Woerner, K. Reimann, and T. Elsaesser, J. Phys.: Condens. Matter **16**, R25 (2004).
[6]A. Wittmann, Y. Bonetti, J. Faist, E. Gini, and M. Giovannini, Appl. Phys. Lett. **93**, 141103 (2008).
[7]H. Choi, L. Diehl, Z.-K. Wu, M. Giovannini, J. Faist, F. Capasso, and T. B. Norris, Phys. Rev. Lett. **100**, 167401 (2008).
[8]H. Risken and K. Nummedal, J. Appl. Phys. **39**, 4662 (1968); R. Graham and H. Haken, Z. Phys. **213**, 420 (1968).
[9]C. R. Menyuk and M. A. Talukder, Phys. Rev. Lett. **102**, 023903 (2009).
[10]M. A. Talukder and C. R. Menyuk, Phys. Rev. A **79**, 063841 (2009).
[11]S. L. McCall and E. L. Hahn, Phys. Rev. Lett. **18**, 908 (1967).
[12]S. L. McCall and E. L. Hahn, Phys. Rev. **183**, 457 (1969).
[13]M. A. Talukder and C. R. Menyuk, Proceedings of the International Quantum Cascade Lasers School and Workshop, Monte Verita, Switzerland, 2008 (unpublished).
[14]M. A. Talukder and C. R. Menyuk, Proceedings of the IEEE LEOS Annual Meeting, Newport Beach, CA, 2008 (unpublished).
[15]L. Allen and J. H. Eberley, *Optical Resonance and Two Level Atoms* (Dover, New York, 1987).
[16]R. W. Boyd, *Nonlinear Optics*, 2nd ed. (Academic, London, 2003).
[17]H. A. Haus, IEEE J. Sel. Top. Quantum Electron. **6**, 1173 (2000).
[18]C. Y. Wang, L. Diehl, A. Gordon, C. Jirauschek, F. X. Kärtner, A. Belyanin, D. Bour, S. Corzine, G. Höfler, M. Troccoli, J. Faist, and F. Capasso, Phys. Rev. A **75**, 031802 (2007).
[19]A. Gordon, C. Y. Wang, L. Diehl, F. X. Kärtner, A. Belyanin, D. Bour, S. Corzine, G. Höfler, H. C. Liu, H. Schneider, T. Maier, M. Troccoli, J. Faist, and F. Capasso, Phys. Rev. A **77**, 053804 (2008).